

# Pressure-induced amorphization and decomposition in $\text{ZrV}_2\text{O}_7$ : A Raman spectroscopic study

T. Sakuntala,<sup>1,\*</sup> A. K. Arora,<sup>2</sup> V. Sivasubramanian,<sup>2</sup> Rekha Rao,<sup>1</sup> S. Kalavathi,<sup>2</sup> and S. K. Deb<sup>1</sup>

<sup>1</sup>High Pressure Physics Division, Bhabha Atomic Research Center, Mumbai 400085, India

<sup>2</sup>Materials Science Division, Indira Gandhi Center for Atomic Research, Kalpakkam 603102, India

(Received 27 November 2006; revised manuscript received 2 February 2007; published 30 May 2007)

*In situ* high-pressure Raman spectroscopic studies on  $\text{ZrV}_2\text{O}_7$  suggest growth of disorder in the high-pressure orthorhombic phase, inferred from the excessive broadening of Raman peaks, and the sample gradually turns amorphous above 4 GPa. The samples pressure cycled from 10 GPa exhibit irreversible amorphization. On the other hand, the spectrum of the sample pressure cycled from 4 GPa is found to have all the characteristic peaks of  $\text{V}_2\text{O}_5$  indicating a possible decomposition of the compound into a mixture of simple oxides. A partial decomposition is indeed confirmed from the x-ray-diffraction pattern of the recovered sample. A large decrease of the intensity of the  $\text{VO}_4$  tetrahedral stretching modes is consistent with the possible coordination change of vanadium, from fourfold in  $\text{ZrV}_2\text{O}_7$  to fivefold in  $\text{V}_2\text{O}_5$ . Nucleation of nano-/poorly crystallized grains of the daughter phase even at ambient temperature is understood as due to the existence of the fivefold coordinated crystalline phase,  $\text{V}_2\text{O}_5$ .

DOI: 10.1103/PhysRevB.75.174119

PACS number(s): 62.50.+p, 64.70.-p, 78.30.-j

## I. INTRODUCTION

Pressure-induced solid-state decomposition of compounds into mixtures of dense-packed daughter phases, reported in many systems such as  $\text{Fe}_2\text{SiO}_4$ ,<sup>1</sup>  $\text{CuGeO}_3$ ,<sup>2</sup>  $\text{Mg}_2\text{SiO}_4$ ,<sup>3</sup>  $\text{Bi}_4(\text{GeO}_4)_3$ ,<sup>4</sup>  $\text{Zr}(\text{WO}_4)_2$ ,<sup>5</sup>  $\text{Sc}_2(\text{MoO}_4)_3$ ,<sup>6</sup>  $\text{Zr}(\text{MoO}_4)_2$ ,<sup>7</sup>  $\text{CO}_2$ ,<sup>8</sup> and  $\text{KHSO}_4$ ,<sup>9</sup> has been found to occur only at elevated temperature, except in  $\text{KHSO}_4$ . This is because the nucleation and growth of macroscopic phases of the daughter compounds require considerable atomic diffusion that is possible only at elevated temperature. Consequently, at ambient temperature, these compounds invariably exhibit pressure-induced amorphization (PIA) as the decomposition is kinetically hindered.<sup>10</sup>  $\text{KHSO}_4$  decomposes at ambient temperature as one of the daughter compounds,  $\text{H}_2\text{SO}_4$ , happened to be liquid.<sup>9</sup> The report of the specific volume of the  $\text{Zr}(\text{WO}_4)_2$  in the pressure-amorphized state being the same as that for a mixture of  $\text{ZrO}_2$  and  $2\text{WO}_3$  strongly suggested that the pressure-amorphized state is a precursor to decomposition.<sup>11</sup> Here, we report the evidence of pressure-induced solid-state decomposition occurring at ambient temperature in  $\text{ZrV}_2\text{O}_7$ , a network structure that exhibits negative thermal expansion above 373 K.

Several network structures such as  $\text{Zr}(\text{WO}_4)_2$ ,<sup>12</sup>  $\text{Zr}(\text{MoO}_4)_2$ ,<sup>13</sup>  $\text{Sc}_2(\text{MoO}_4)_3$ ,<sup>6</sup>  $\text{Sc}_2(\text{WO}_4)_3$ ,<sup>14</sup>  $\text{Lu}_2(\text{WO}_4)_3$ ,<sup>15</sup> and  $\text{Y}_2(\text{WO}_4)_3$  (Ref. 16) that exhibit negative thermal expansion (NTE) are found to undergo amorphization at high pressure. Although a correlation between the NTE and PIA has often been mentioned,<sup>14,15,17-19</sup> another network structure  $\text{Al}_2(\text{WO}_4)_3$  that shows positive thermal expansion also undergoes PIA.<sup>20</sup> In this context, it is of interest to examine other similar network structures such as  $\text{ZrV}_2\text{O}_7$  (Refs. 21 and 22) and  $\text{HfV}_2\text{O}_7$  (Ref. 23) that exhibit PIA. The high-temperature cubic phase of  $\text{ZrV}_2\text{O}_7$  bears structural similarities with the cubic  $\text{Zr}(\text{WO}_4)_2$  and exhibits NTE.<sup>24</sup> Instead of separated pairs of  $\text{WO}_4$  ions, here, two  $\text{VO}_4$  tetrahedra share an oxygen atom at a common vertex to form  $\text{V}_2\text{O}_7$  structural unit. Consequently, the main difference with respect to zirconium tungstate is that all the corners of the polyhedra are

corner linked, leaving no nonbridging (terminal) oxygen atoms.<sup>25</sup> At room temperature, the structure is a  $3 \times 3 \times 3$  supercell of the high-temperature phase and exhibits positive thermal expansion. Recently, powder x-ray-diffraction studies of a related compound  $\text{HfV}_2\text{O}_7$  at high pressure revealed that the diffraction intensities corresponding to the parent phase become weak over the pressure range 3.3–4.0 GPa along with the appearance of a new set of peaks; however, the transformation was rather incomplete leading to a gradual loss of long-range order.<sup>23</sup> Earlier, high-pressure x-ray powder-diffraction studies of  $\text{ZrV}_2\text{O}_7$  have shown that above 1.4 GPa, the compound exhibits transition to an orthorhombic structure,<sup>21</sup> and subsequently becomes amorphous above 4 GPa. The high-pressure phases have not been examined using Raman spectroscopy, which is a useful technique for probing disorder of structural units and for identifying presence of different chemical compositions, even if the transformation is only partial.<sup>9</sup> In this work, we report the results of *in situ* high-pressure Raman spectroscopic study of  $\text{ZrV}_2\text{O}_7$ , synthesized using solid-state reaction method. The Raman spectra of the samples recovered after pressure cycling to different pressures are compared with those of the starting sample and  $\text{V}_2\text{O}_5$ . X-ray-diffraction pattern of the sample recovered after pressure cycling to 4 GPa is analyzed for possible presence of decomposition products such as  $\text{V}_2\text{O}_5$  and  $\text{ZrO}_2$ . The occurrence of pressure-induced decomposition in this system at ambient temperature is discussed in terms of existence of crystalline phases with higher coordination number.

## II. EXPERIMENTAL DETAILS

Zirconium vanadate was synthesized by solid-state reaction method using stoichiometric mixture of  $\text{ZrO}_2$  (purity 99.99%) and  $\text{V}_2\text{O}_5$  (99.8%). The mixture was initially calcined at 700 °C for 72 h with several intermittent grinding. Final calcination was carried out at 750 °C for 24 h. The x-ray-diffraction pattern was recorded using STOE diffractometer using  $\text{Cu K}\alpha$  radiation. Raman-scattering measure-

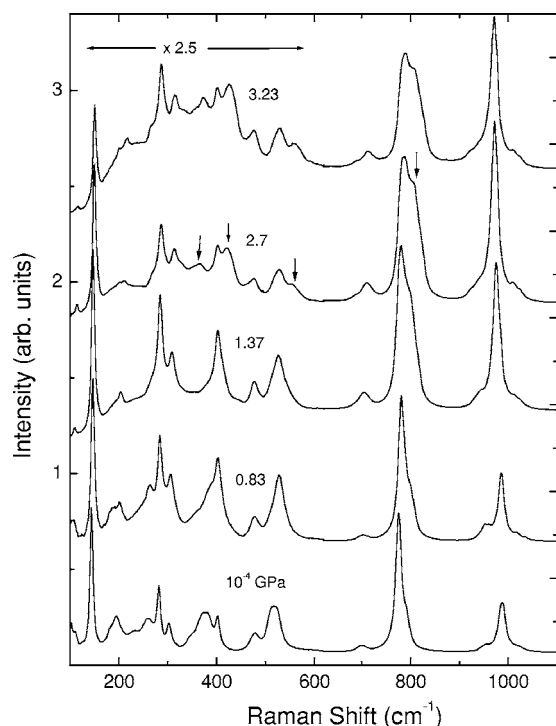


FIG. 1. Raman spectra of  $\text{ZrV}_2\text{O}_7$  at various pressures. Intensities in the range  $100\text{--}620\text{ cm}^{-1}$  have a scale factor of 2.5 and vertically shifted. Arrows indicate the modes that gain in intensity in the orthorhombic phase above 1.4 GPa.

ments at high pressure were carried out using a diamond-anvil cell (DAC), Diacell Products, UK, Model B-05. A 4:1 methanol-ethanol mixture was used as pressure transmitting medium. The pressure inside the cell was measured using the standard ruby fluorescence technique. Raman spectrum of polycrystalline  $\text{ZrV}_2\text{O}_7$  from inside the DAC was excited using 532 nm line of power  $\sim 15$  mW. Scattered light was analyzed using a homebuilt 0.9 m single monochromator, coupled with a super notch filter and detected by a cooled charge coupled device (Andor Technology). The entrance slit is kept at  $50\text{ }\mu\text{m}$ , which gives a spectral bandpass of  $3\text{ cm}^{-1}$ .

### III. RESULTS AND DISCUSSION

X-ray-diffraction pattern confirmed the formation of a single-phase material and it could be fitted to a cubic unit cell with a lattice parameter of  $8.774(3)\text{ \AA}$ , in good agreement with the reported value of  $8.777\text{ \AA}$ .<sup>24</sup> Figure 1 shows the evolution of Raman spectrum of  $\text{ZrV}_2\text{O}_7$  at high pressures. The lowest-frequency mode observed in the present studies appears around  $144\text{ cm}^{-1}$ . In the spectral range  $180\text{--}580\text{ cm}^{-1}$ , there are several overlapping Raman bands and could be fitted to 11 distinct bands at ambient conditions using Lorentzian line-shape function. The high-frequency range between  $680$  and  $1100\text{ cm}^{-1}$  was fitted to five bands centered around  $699$ ,  $775$ ,  $792$ ,  $987$ , and  $1020\text{ cm}^{-1}$  at ambient conditions. Around 1.4 GPa, the pressure corresponding to the reported cubic-orthorhombic transition,<sup>21</sup> intensities of some of the bands such as those around  $260$  and  $383\text{ cm}^{-1}$  reduce while new modes around  $365$ ,  $418$ , and  $545\text{ cm}^{-1}$

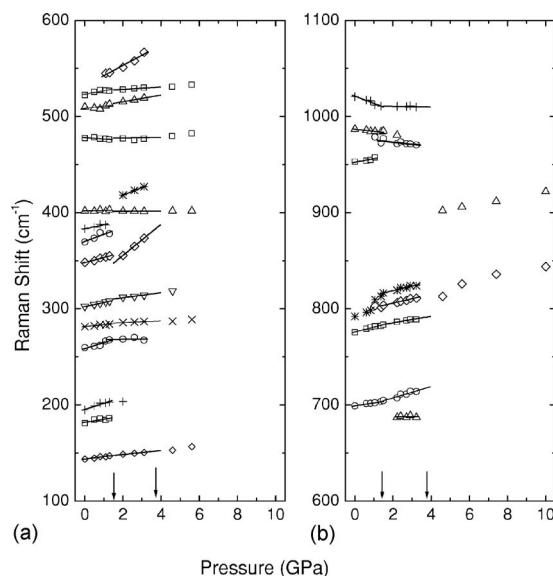


FIG. 2. (a),(b) Pressure dependence of mode frequencies in  $\text{ZrV}_2\text{O}_7$ . The solid lines are linear fit to the data. Many new modes appear and some of the modes corresponding to the cubic phase decrease in intensity and could not be observed above the phase-transition pressure of 1.4 GPa. Arrows indicate transition pressures corresponding to the orthorhombic and amorphous phases.

grow in intensity. In the high-frequency region, there is a noticeable change in the relative intensities of the  $775$  and  $987\text{ cm}^{-1}$  bands (Fig. 1). These spectral changes are gradual unlike in  $\text{ZrW}_2\text{O}_8$  (Ref. 1) wherein the Raman spectrum changes abruptly across the cubic-orthorhombic transition. It may be recalled that in the case of  $\text{ZrW}_2\text{O}_8$ , this transition involves tilting of the  $\text{WO}_4$  tetrahedra<sup>26</sup> off the threefold axis together with the inversion of one-third of the  $\text{W}_2\text{O}_8$  units. This transition is also accompanied by a volume change of about 5%.<sup>26</sup> However, in  $\text{ZrV}_2\text{O}_7$ , x-ray-diffraction studies<sup>21</sup> showed that the volume discontinuity across this transition is rather small, about 0.88%.<sup>27</sup> This is perhaps the reason for less pronounced discontinuities in the phonon spectrum as compared to zirconium tungstate. Figure 2 shows the pressure dependence of mode frequencies in  $\text{ZrV}_2\text{O}_7$ . One can see that most of the mode frequencies increase with increasing pressure. The V-O stretching band around  $987\text{ cm}^{-1}$  and the weak sideband at  $1020\text{ cm}^{-1}$  decrease in frequency with an increase in pressure and can be understood as due to an increase in V-O bond length evolving toward a higher coordination. A few modes in the tetrahedral V-O bending mode region between  $400$  and  $550\text{ cm}^{-1}$  are found to be weakly dependent on pressure. In particular, the mode at  $476\text{ cm}^{-1}$  has a weak negative slope of  $-1.3\text{ cm}^{-1}/\text{GPa}$  in the cubic phase, implying softening of O-V-O bending force constants. Some of the modes show significant changes in the pressure dependence of mode frequencies across cubic-orthorhombic phase transition at 1.4 GPa, as may be noted from Fig. 2. There is a continuous evolution of Raman intensities in the orthorhombic phase (Fig. 1). At pressures around 3.9 GPa, most of the Raman bands corresponding to the parent phase disappear abruptly, consistent with the reported amorphization pressure.<sup>21</sup> Figure 3 shows the typical Raman spectra at

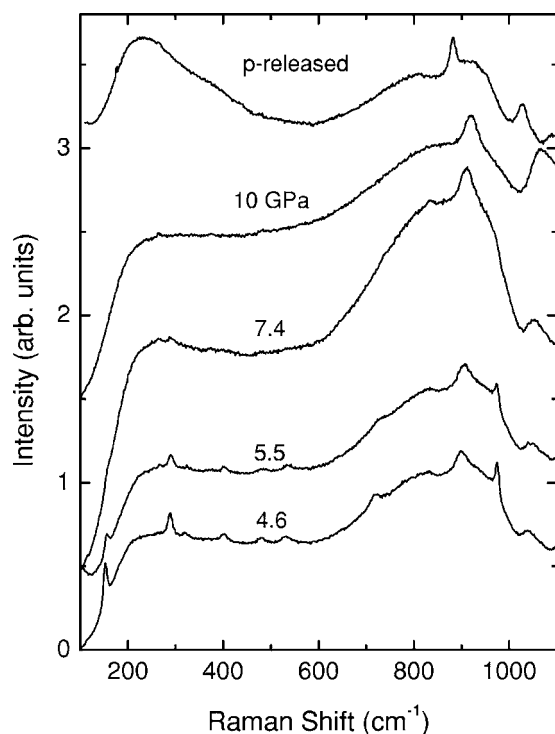


FIG. 3. Raman spectrum of  $\text{ZrV}_2\text{O}_7$  at various pressures in the amorphous phase above 4 GPa.

pressures above 4 GPa. A very broad band (full width at half maximum more than  $300\text{ cm}^{-1}$ ) centered around  $800\text{ cm}^{-1}$  is observed in the high-frequency region. A few sharp features can be seen riding on the broad background, which become too weak to be observed upon further pressurization up to 10 GPa. The pressure-released spectrum resembles that of the amorphous phase of the compound.

In a few other pressure runs, in which the pressure was reduced from about 4 to 5 GPa, Raman spectrum showed features of a relatively ordered phase upon reducing the pressure. Figure 4 shows the Raman spectrum of the compound in which the pressure is reduced from about 4 GPa, that is, just above the amorphization pressure. Upon reducing the pressure from 4 GPa, one can see that the lower-frequency region of the spectrum showed relatively narrow peaks, while the higher-frequency region exhibited broad bands. It is found that while the spectrum of the pressure-cycled sample has some bands matching with those of the parent compound, there are also some differences. The bands around  $260$ ,  $345$ , and  $370\text{ cm}^{-1}$  in curve (a) are not observed in (c) and a very large reduction in the intensity of the  $775\text{ cm}^{-1}$  mode is noted in the high-frequency region. In fact, the spectrum in the range  $100\text{--}740\text{ cm}^{-1}$  closely resembles that of  $\text{V}_2\text{O}_5$ ,<sup>28</sup> which is also shown in Fig. 4 for the sake of comparison. The peaks in the low- and high-frequency regions appear to be riding over a background similar to that found for the amorphized sample.

In the context of catalysis,  $\text{V}_2\text{O}_5\text{-ZrO}_2$  system has been extensively studied using spectroscopic technique.<sup>29</sup> Formation of  $\text{ZrV}_2\text{O}_7$  from the mixture of  $\text{ZrO}_2$  and  $\text{V}_2\text{O}_5$  at temperatures above  $873\text{ K}$  is characterized by the appearance of the modes at  $260$ ,  $370$ , and  $775\text{ cm}^{-1}$ .<sup>29</sup> In the present work,

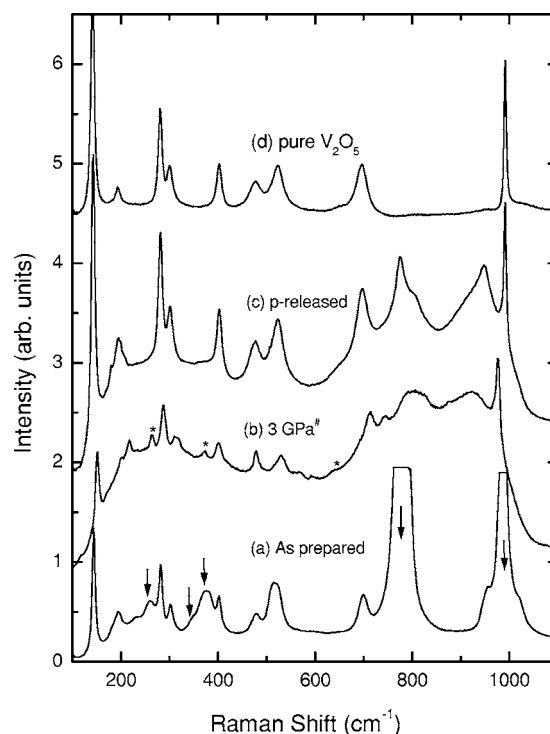


FIG. 4. Raman spectrum of  $\text{ZrV}_2\text{O}_7$ : (a) as synthesized, (b) at 3 GPa in  $p$ -reducing cycle after reaching 4 GPa, (c) at ambient after  $p$  released from 4 GPa, and (d) pure  $\text{V}_2\text{O}_5$ . # indicates spectrum recorded in the  $p$ -reducing cycle. Arrows in (a) represent the peaks that are unique to  $\text{ZrV}_2\text{O}_7$  and are absent or drastically reduced in intensity in the pressure-cycled compound. In curve (b), \* indicate the position of Raman peaks corresponding to  $t\text{-ZrO}_2$ .

it is the same set of modes that disappear/reduce drastically in intensity in the pressure-cycled samples. The broad feature centered around  $790\text{ cm}^{-1}$  [curve (b), Fig. 4] that has been identified to be due to  $\text{Zr-O-V}$  vibrations<sup>29</sup> suggests that these linkages are highly disordered. The overall matching of the spectrum of the pressure-cycled sample with that of  $\text{V}_2\text{O}_5$  suggests decomposition of  $\text{ZrV}_2\text{O}_7$  into  $\text{V}_2\text{O}_5$  and possibly  $\text{ZrO}_2$ . It may be pointed out that in  $\text{V}_2\text{O}_5$ , the highest-frequency mode (V-O stretching) at  $996\text{ cm}^{-1}$  has a typical width of  $6\text{ cm}^{-1}$  at ambient conditions. On the other hand, in  $\text{ZrV}_2\text{O}_7$ , this peak appears at  $987\text{ cm}^{-1}$  and has a larger width of  $\sim 18\text{ cm}^{-1}$ . The sharp band observed at  $996\text{ cm}^{-1}$  in the pressure-cycled sample has a narrow linewidth ( $8\text{ cm}^{-1}$ ) compared to that in  $\text{ZrV}_2\text{O}_7$ , suggesting that it is indeed due to  $\text{V}_2\text{O}_5$ .

In order to confirm the decomposition of  $\text{ZrV}_2\text{O}_7$  at high pressure, *ex situ* x-ray-diffraction measurements were also carried out. The compound was subjected to a compressive stress of  $\sim 4.6\text{ GPa}$  in a conventional opposed-anvil apparatus. The Raman spectrum of the sample recovered after pressure release was found to be similar to that of curve (c) in Fig. 4, except for a somewhat larger fraction of  $\text{ZrV}_2\text{O}_7$ , inferred from the intensity of the  $775\text{ cm}^{-1}$  mode. Figure 5 shows the x-ray-diffraction patterns of the as-synthesized and pressure-cycled samples. One can see that the recovered pattern has, in addition to the diffraction peaks of  $\text{ZrV}_2\text{O}_7$ , also the peaks corresponding to those of  $\text{V}_2\text{O}_5$  and tetragonal

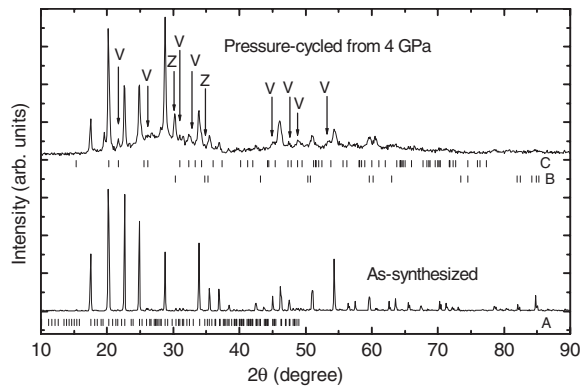


FIG. 5. Powder x-ray-diffraction pattern of  $\text{ZrV}_2\text{O}_7$  recorded using  $\text{Cu K}\alpha$  radiation; (a) as synthesized and (b) sample recovered after pressure cycling to about 4.5 GPa. The tick patterns A, B, and C correspond to JCPDS data for  $\text{ZrV}_2\text{O}_7$  (Ref. 45: calculated pattern only up to  $49^\circ$ ), tetragonal  $\text{ZrO}_2$  (Ref. 46), and  $\text{V}_2\text{O}_5$  (Ref. 47), respectively.  $3 \times 3 \times 3$  supercell  $\text{ZrV}_2\text{O}_7$  has a large number of weak ( $<0.5\%$  intensity) superlattice reflections as evident in the tick pattern. The intense peaks are essentially those of the smaller cubic cell. The peaks labeled as V and Z in the recovered pattern correspond to those of  $\text{V}_2\text{O}_5$  and tetragonal  $\text{ZrO}_2$ , respectively. Note that some of the intense peaks such as the one around  $2\theta = 20.2, 33.9$  can be indexed to both  $\text{ZrV}_2\text{O}_7$  and  $\text{V}_2\text{O}_5$ .

$\text{ZrO}_2$  ( $t\text{-ZrO}_2$ ), confirming a partial decomposition of  $\text{ZrV}_2\text{O}_7$ . The width of the diffraction lines in the pressure-cycled sample is found to be more compared to that of the as-synthesized sample, suggesting small crystallite sizes of the pressure-cycled sample. In addition, an amorphouslike background centered around  $28^\circ$  also appears to be present. Thus, the pressure-cycled sample appears to be a mixture of the parent compound,  $\text{V}_2\text{O}_5$ ,  $t\text{-ZrO}_2$ , and also amorphous  $\text{ZrV}_2\text{O}_7$ . It may also be pointed out that in the earlier x-ray studies, while the diffraction intensities of the parent phase reduced drastically around 3.9 GPa, new weak peaks were indeed observed even up to 6.4 GPa [Fig. 1(a) in Ref. 21], suggesting poorly formed crystalline phase, different from that of the parent compound. This is consistent with the present observation, namely, the presence of some crystalline-like Raman peaks even in the amorphous phase at 4.6 GPa (Fig. 3); frequencies of which are very close to those of  $\text{V}_2\text{O}_5$ , indicating traces of poorly crystallized  $\text{V}_2\text{O}_5$ . Formation of  $t\text{-ZrO}_2$  rather than the monoclinic phase in the pressure-cycled sample may be due to the small crystallite size, as the  $t\text{-ZrO}_2$  is known to be stable in sizes less than about 30 nm.<sup>30</sup> The weak Raman bands at 262 and  $640\text{ cm}^{-1}$  in curve (b) of Fig. 4 closely match with the Raman bands expected for  $t\text{-ZrO}_2$ .<sup>31</sup> Poorly crystallized  $\text{ZrO}_2$  is known to exhibit a broad peak in the range  $300\text{--}600\text{ cm}^{-1}$  and is attributed to a mixture of monoclinic and tetragonal  $\text{ZrO}_2$  phases.<sup>28</sup>

Several reasons have been considered for understanding pressure-induced structural transitions, such as mechanical instability.<sup>32,33</sup> One of them is the repulsive contribution to free energy from nonbonded interactions.<sup>34</sup> This factor is known to be relevant in the temperature-driven transition in  $\text{ZrV}_2\text{O}_7$ ; one of the reasons is to avoid certain short O-O distances.<sup>22</sup> Such unfavorable nonbonded distances/

interpolyhedral angles could also arise under compression. Many of the systems that show negative thermal expansion and a tendency for PIA are also reported to have larger compressibilities, often resulting in short nonbonded distances at moderate pressures. For example, in  $\text{ZrV}_2\text{O}_7$ , the volume reduction even at 4 GPa is about 15%, whereas for  $\text{TiP}_2\text{O}_7$  and  $\text{ZrP}_2\text{O}_7$ , which do not exhibit PIA, these values are 6% and 8%, respectively.<sup>21</sup> Rapid increase in the repulsive contribution due to nonbonded interactions is quite possibly driving the system to transform into structures of smaller volumes/larger coordination. Decomposition of  $\text{ZrV}_2\text{O}_7$  at high pressure may be rationalized from the volume change considerations.<sup>4</sup> At ambient conditions, the volume of  $\text{ZrV}_2\text{O}_7$  per f.u. is  $169\text{ \AA}^3$ , whereas for the monoclinic  $\text{ZrO}_2$  and orthorhombic  $\text{V}_2\text{O}_5$ , these values are  $35.06$  and  $89.6\text{ \AA}^3$ , respectively. The fractional decrease in volume upon decomposition  $[V_{\text{ZV}} - (V_{\text{Z}} + V_{\text{V}})]/V_{\text{ZV}}$  turns out to be quite large, about 26%. Here,  $V_{\text{ZV}}$ ,  $V_{\text{Z}}$ , and  $V_{\text{V}}$  denote the volume of zirconium vanadate,  $m\text{-ZrO}_2$ , and  $\text{V}_2\text{O}_5$ , respectively. The  $t\text{-ZrO}_2$  has a slightly smaller volume compared to  $m\text{-ZrO}_2$ . For  $\text{ZrV}_2\text{O}_7$ , reduction in volume upon compression to 4 GPa, estimated from compressibility data, is only 15% which implies that at 4 GPa, the daughter products would still have volume much smaller compared to the parent compound. Decomposition at high pressure is also favorable from coordination considerations.  $\text{V}_2\text{O}_5$  has a layered structure made up of edge- and corner-sharing  $\text{VO}_5$  square pyramids,<sup>35</sup> whereas in the monoclinic  $\text{ZrO}_2$ , Zr atoms have sevenfold oxygen coordination.<sup>36</sup> Studies on the evolution of the local structure of  $\text{ZrW}_2\text{O}_8$  in the high-pressure orthorhombic phase<sup>37</sup> revealed that the W-O bond length increased continuously to accommodate higher W-O coordination. However, decomposition in other tungstates and molybdates does not occur at ambient temperature close to the amorphization pressure because the decomposition products ( $\text{WO}_3$  and  $\text{MoO}_3$ ) exist in only sixfold coordinated crystalline phases. On the other hand, existence of a fivefold coordinated crystalline phase of  $\text{V}_2\text{O}_5$  facilitates its occurrence at ambient temperature in zirconium vanadate. In the present case, the decrease in the frequency of the  $987\text{ cm}^{-1}$  mode in  $\text{ZrV}_2\text{O}_7$  strongly points toward the tendency for increased coordination. In short, the local atomic coordination in  $\text{ZrV}_2\text{O}_7$  around 4 GPa being favorable for formation of  $\text{V}_2\text{O}_5$  appears to be the important factor for decomposition.

The question, why decomposition does not proceed further when the pressure is increased beyond 4 GPa, still remains to be understood. While solid-state decomposition at high pressures is as such kinetically hindered at ambient temperature,<sup>10</sup> stability of the new daughter phases under these conditions is another factor, which could be responsible for decomposition not proceeding at much higher pressures. High-pressure behavior of  $m\text{-ZrO}_2$  has shown that above 4 GPa, the system undergoes a transition to a new orthorhombic phase.<sup>38</sup> Many vanadium oxide-based systems that have  $\text{VO}_4$  structural units, as in the case of  $\text{Ca}_3(\text{VO}_4)_2$ ,<sup>39</sup>  $\text{Sr}_3(\text{VO}_4)_2$ ,  $\text{Ba}_3(\text{VO}_4)_2$ ,<sup>40</sup>  $\text{LiVO}_3$ ,<sup>41</sup> etc., have been reported to become disordered/amorphous under the application of pressure due to impeded transition to a sixfold coordinated structure. High-pressure investigations of  $\text{V}_2\text{O}_5$  by Loa *et*

*al.*<sup>42</sup> have shown that the compound exhibits a transition to a highly disordered phase around 7 GPa, evolving toward a sixfold coordinated structure. One may expect that decomposition from a point wherein the average V-O coordination is 5 would be easier than from a point where the average coordination is 6. In fact, Suzuki *et al.*<sup>43</sup> have shown that crystallization temperature of the orthorhombic  $V_2O_5$  starting from splat-cooled glassy  $V_2O_5$  increases with increasing pressure. The reason for the irreversibility of amorphous phase when  $p$  cycled from higher pressures could thus be related to a larger barrier for formation of  $VO_5$ -like structural units from  $VO_6$  octahedra. Recently, ultrasonic studies have shown softening of elastic constants of zirconium tungstate at high pressure.<sup>44</sup> This essentially implies instability of the structure against a structural phase transition. As both  $ZrW_2O_8$  and  $ZrV_2O_7$  undergo cubic-orthorhombic transition at high pressure, it is likely that  $ZrV_2O_7$  may also exhibit similar softening. The network structures that exhibit NTE invariably have lots of empty spaces between the polyhedral structural units and consequently are loosely packed and have significantly lower density as compared to the oxides from which they are synthesized. Hence, at high pressure, the decomposition of the network structure into a mixture of dense-packed simple oxides becomes energetically favorable. The present results also support this argument.

#### IV. SUMMARY AND CONCLUSIONS

Raman spectroscopic studies have been carried out on  $ZrV_2O_7$  up to 10 GPa, confirming irreversible pressure-induced amorphization of the compound above 4 GPa. On the other hand, when the pressure is reduced from just above the amorphization pressure, the Raman spectrum of the pressure-cycled sample shows evidence for decomposition of the compound into  $V_2O_5$  and  $ZrO_2$ . Decomposition is also confirmed from the *ex situ* x-ray-diffraction measurements, and the products are identified to be  $V_2O_5$  and tetragonal  $ZrO_2$ . These results strongly suggest that in  $ZrV_2O_7$ , pressure-induced amorphization is indeed driven by kinetically hindered decomposition. Though pressure-induced solid-state decomposition usually requires elevated temperature,  $ZrV_2O_7$  appears to be unique that a partial decomposition proceeds even at ambient temperature. The decomposition at ambient temperature is believed to have been facilitated by the existence of a fivefold coordinated crystal-line phase of the daughter product  $V_2O_5$ .

#### ACKNOWLEDGMENTS

The authors are thankful to Alka B. Garg and S. Meenakshi for the opposed-anvil experiments and S. M. Sharma for encouragement.

\*Corresponding author. Electronic address: sakuntl@barc.gov.in

- <sup>1</sup>W. A. Bassett and L. C. Ming, *Phys. Earth Planet. Inter.* **6**, 154 (1972).
- <sup>2</sup>W. Hegensbart, F. Rau, and K. J. Range, *Mater. Res. Bull.* **16**, 413 (1981).
- <sup>3</sup>T. Kato, T. Kubo, H. Morishima, E. Ohtani, A. Suzuki, D. Yamazaki, K. Mibe, T. Kikegawa, and O. Shimomura, *Rev. High Pressure Sci. Technol.* **7**, 119 (1998).
- <sup>4</sup>A. K. Arora, T. Yagi, N. Miyajima, and R. Gopalakrishnan, *J. Phys.: Condens. Matter* **16**, 8117 (2004).
- <sup>5</sup>J. M. G. Amores, U. Amador, E. Moran, and M. A. A. Franco, *Int. J. Inorg. Mater.* **2**, 123 (2000).
- <sup>6</sup>A. K. Arora, T. Yagi, N. Miyajima, and T. A. Mary, *J. Appl. Phys.* **97**, 013508 (2005).
- <sup>7</sup>A. Grzechnik and W. A. Crichton, *Solid State Sci.* **4**, 1137 (2002).
- <sup>8</sup>O. Tschauer, H. K. Mao, and R. J. Hemley, *Phys. Rev. Lett.* **87**, 075701 (2001).
- <sup>9</sup>A. K. Arora and T. Sakuntala, *High Press. Res.* **17**, 1 (2000).
- <sup>10</sup>A. K. Arora, *Solid State Commun.* **115**, 665 (2000).
- <sup>11</sup>A. K. Arora, V. S. Sastry, P. Ch. Sahu, and T. A. Mary, *J. Phys.: Condens. Matter* **16**, 1025 (2004).
- <sup>12</sup>T. R. Ravindran, A. K. Arora, and T. A. Mary, *Phys. Rev. Lett.* **84**, 3879 (2000).
- <sup>13</sup>D. V. S. Muthu, B. Chen, J. M. Wrobel, A. M. K. Anderson, S. Carlson, and M. B. Kruger, *Phys. Rev. B* **65**, 064101 (2002).
- <sup>14</sup>R. A. Secco, H. Liu, N. Imanaka, and G. Adachi, *J. Mater. Sci. Lett.* **20**, 1339 (2001).
- <sup>15</sup>H. Liu, R. A. Secco, N. Imanaka, and G. Adachi, *Solid State Commun.* **121**, 177 (2002).

- <sup>16</sup>S. Karmakar, S. K. Deb, A. K. Tyagi, and S. M. Sharma, *J. Solid State Chem.* **177**, 4087 (2004).
- <sup>17</sup>R. J. Speedy, *J. Phys.: Condens. Matter* **8**, 10907 (1996).
- <sup>18</sup>C. A. Perottoni and J. A. H. da Jornada, *Science* **280**, 886 (1998).
- <sup>19</sup>S. K. Sikka, *J. Phys.: Condens. Matter* **16**, S1033 (2004).
- <sup>20</sup>N. Garg, V. Panchal, A. K. Tyagi, and S. M. Sharma, *J. Solid State Chem.* **178**, 998 (2005).
- <sup>21</sup>S. Carlson and A. M. K. Anderson, *J. Appl. Crystallogr.* **34**, 7 (2001).
- <sup>22</sup>R. L. Withers, J. S. O. Evans, J. Hanson, and A. W. Sleight, *J. Solid State Chem.* **137**, 161 (1998).
- <sup>23</sup>U. L. C. Hemamala, F. El-Ghoussein, A. M. Goedken, B. Chen, Ch. Leroux, and M. B. Kruger, *Phys. Rev. B* **70**, 214114 (2004).
- <sup>24</sup>A. K. A. Pryde, K. D. Hammonds, M. T. Dove, V. Heine, J. D. Gale, and M. C. Warren, *J. Phys.: Condens. Matter* **8**, 10973 (1996).
- <sup>25</sup>N. Khosrovani, A. W. Sleight, and T. Vogt, *J. Solid State Chem.* **132**, 355 (1997).
- <sup>26</sup>J. D. Jorgensen, Z. Hu, S. Teslic, D. N. Argyriou, S. Short, J. S. O. Evans, and A. W. Sleight, *Phys. Rev. B* **59**, 215 (1999).
- <sup>27</sup>From the tabulated values of cell parameters at various pressures (Ref. 18), volumes of  $ZrV_2O_7$  in the cubic phase at 1.38 GPa and the orthorhombic phase at 1.58 GPa were calculated to be 622.0 and 610.5 Å<sup>3</sup>, respectively. Extrapolated volume of the cubic phase at 1.58 GPa is 615 Å<sup>3</sup> and the discontinuity at 1.58 GPa is estimated to be 0.88%.
- <sup>28</sup>J. R. Sohn, J. S. Han, and J. S. Lim, *Mater. Chem. Phys.* **91**, 558 (2005).
- <sup>29</sup>L. L. Male, H. G. Niessen, A. T. Bell, and T. D. Tilley, *J. Catal.* **194**, 431 (2000).

- <sup>30</sup>G. Baldinozzi, D. Simeone, D. Gosset, and M. Dutheil, *Phys. Rev. Lett.* **90**, 216103 (2003).
- <sup>31</sup>T. Merle, R. Guinebretiere, A. Mirgorodsky, and P. Quintard, *Phys. Rev. B* **65**, 144302 (2002).
- <sup>32</sup>F. Sciortino, U. Essmann, H. E. Stanley, M. Hemmati, J. Shao, G. H. Wolf, and C. A. Angell, *Phys. Rev. E* **52**, 6484 (1995).
- <sup>33</sup>N. Choudhury and S. L. Chaplot, *Phys. Rev. B* **73**, 094304 (2006).
- <sup>34</sup>S. K. Sikka and S. M. Sharma, *Curr. Sci.* **63**, 317 (1992).
- <sup>35</sup>R. Enjalbert and J. Galy, *Acta Crystallogr., Sect. C: Cryst. Struct. Commun.* **C42**, 1467 (1986).
- <sup>36</sup>D. K. Smith and H. W. Newkirk, *Acta Crystallogr.* **18**, 983 (1965).
- <sup>37</sup>T. Varga, A. P. Wilkinson, A. C. Jupe, C. Lind, W. A. Basset, and C.-S. Zha, *Phys. Rev. B* **72**, 024117 (2005).
- <sup>38</sup>O. Ohtaka, H. Fukui, T. Kunisada, T. Fujisawa, K. Funakoshi, W. Utsumi, T. Irifune, K. Kuroda, and K. Kikegawa, *Phys. Rev. B* **63**, 174108 (2001).
- <sup>39</sup>A. Grzechnik, *Solid State Chem.* **139**, 161 (1998).
- <sup>40</sup>A. Grzechnik and P. F. McMillan, *J. Solid State Chem.* **132**, 156 (1997).
- <sup>41</sup>Z. X. Shen, C. W. Ong, M. H. Kuok, and S. H. Tang, *J. Phys.: Condens. Matter* **7**, 939 (1995).
- <sup>42</sup>I. Loa, A. Grzechnik, U. Schwarz, K. Syassen, M. Hanfland, and R. K. Kremer, *J. Alloys Compd.* **317**, 103 (2001).
- <sup>43</sup>T. Suzuki, S. Saito, and W. Arakawa, *J. Non-Cryst. Solids* **24**, 355 (1977).
- <sup>44</sup>C. Pantea, A. Migliori, P. B. Littlewood, Y. Zhao, H. Ledbetter, J. C. Lashley, T. Kimura, J. Van Duijn, and G. R. Kowach, *Phys. Rev. B* **73**, 214118 (2006).
- <sup>45</sup>Powder Diffraction File, Card No. 87-0562, JCPDS (International Center for Diffraction Data, Newton Square, Pennsylvania).
- <sup>46</sup>Powder Diffraction File, Card No. 50-1089, JCPDS (International Center for Diffraction Data, Newton Square, Pennsylvania).
- <sup>47</sup>Powder Diffraction File, Card No. 41-1426, JCPDS (International Center for Diffraction Data, Newton Square, Pennsylvania).